

Interference Mitigation In Wireless Mesh Networks Through Radio Co-location Aware Conflict Graphs

Srikant Manas Kala*, Ranadheer Musham, M Pavan Kumar Reddy, Bheemarjuna Reddy Tamma

Indian Institute of Technology Hyderabad, India

Email:[*cs12m1012, cs12b1026, cs12b1025, tbr]@iith.ac.in

arXiv:1412.2566v3 [cs.NI] 16 Mar 2015

Abstract—The emergence of Wireless Mesh Networks (WMNs) as a prospective wireless communication technology of immense interest, has also inadvertently spawned a plethora of network bottlenecks caused by the interference endemic in such wireless networks. Conflict Graphs are indispensable tools to theoretically represent and estimate this interference. We propose a broad-based and generic algorithm to generate conflict graphs, which is independent of the underlying interference model. Further, we propose the notion of radio co-location interference, caused and experienced by spatially co-located radios, installed on adjacent nodes in multi-radio multi-channel (MRMC) WMNs. We experimentally validate the concept, and propose a new all-encompassing algorithm, to create a radio co-location aware Conflict Graph. Our novel conflict graph generation algorithm is demonstrated to be significantly superior, and more efficient, than the conventional approach, both theoretically and experimentally. The results of an extensive set of ns-3 simulations, run on the IEEE 802.11 platform, strongly indicate that the radio co-location aware conflict graphs are a marked improvement over their conventional counterparts. We also question the use of *total interference degree* as a reliable metric to gauge or predict WMN performance, especially in context to the channel-assignment schemes, based on our results and findings.

1. INTRODUCTION

Wireless Mesh Networks have emerged as a promising technology, with a potential for widespread application in contemporary wireless networks, substituting and thereby reducing

the dependence on the wired infrastructure. It is fathomable that in the foreseeable future, WMNs may be extensively deployed due to consistently increasing low-cost availability of the commodity IEEE 802.11 off-the-shelf hardware, smooth deployment with ease of scalability, effortless reconfigurability and increased network coverage [1] [2]. The surge in their presence will be equally attributed to the tremendous increase in data communication rates that are being guaranteed by the IEEE 802.11 and IEEE 802.16 protocol standards. WMNs also offer enhanced reliability when compared to their wired counterparts because of the inherent redundancy in the underlying mesh topology. WMN technology, given its practical and commercial appeal, can adequately cater to the vigorous needs of myriad network applications, ranging from institutional and social wireless LANs, last-mile broadband Internet access, to disaster networks. Prominent wireless technologies that stand to benefit, or are already benefiting from WMN deployments, other than the IEEE 802.11 WLANs, are the IEEE 802.16 Wireless Metropolitan Area Networks (WMANs) and the next generation cellular mobile systems, including LTE-Advanced [3]. WMNs are also poised to form the backbone of the next-generation of integrated wireless networks, that aim to converge a plethora of technologies such as 3G/4G mobile networks, WLANs etc. onto a single communication delivery platform [4].

The mesh topology framework in a WMN facilitates multiple-hop transmissions to relay the data traffic seamlessly between source-destination pairs that are often beyond the transmission range of each other [5]. Thus each node in the *Wireless Mesh Backbone* acts as a host and as a router, forwarding packets onto the next hop. A WMN deployment can provide both, a self-contained IEEE 802.11 WLAN with no connectivity to foreign networks, as well as an unrestricted access to outside networks, or broadband access to the Internet, through a Gateway. Several Gateways may be required if the WMN has to establish communication links with external networks. A simplistic WMN architecture is constituted of numerous mesh-routers (hereafter, referred to as nodes), which relay/route the data traffic via multiple-hop transmissions and leverage the twin WMN features of being fully wireless and having a mesh topology. The mesh-clients are the ultimate end-user devices that are serviced by the WMN backbone of mesh-routers. Gateways exhibit operational duality by interfacing the WMN with outside networks, besides functioning as any other mesh router within the WMN. IEEE 802.11 [6] protocol standards serve as a popular link layer protocol for WMN deployment. A trivial single-gateway WMN is illustrated in Figure 1, with mesh-routers and mesh-clients. This is the WMN model we adhere to in our research endeavor, wherein we consider the availability of multiple radios specifically for inter mesh-router communication, and do not deal with the mesh backbone to mesh-client communication issues.

Initial deployments of WMNs comprised of a trivial single-radio single-channel architecture, in which all nodes were equipped with a single radio and assigned the same channel. Subsequent analysis of the performance of such wireless network architectures, revealed that there was substantial degradation in the performance of the network, as the size of the WMN was scaled up [7]. Single-channel deployments also adversely affected the end-to-end throughput and network capacity in

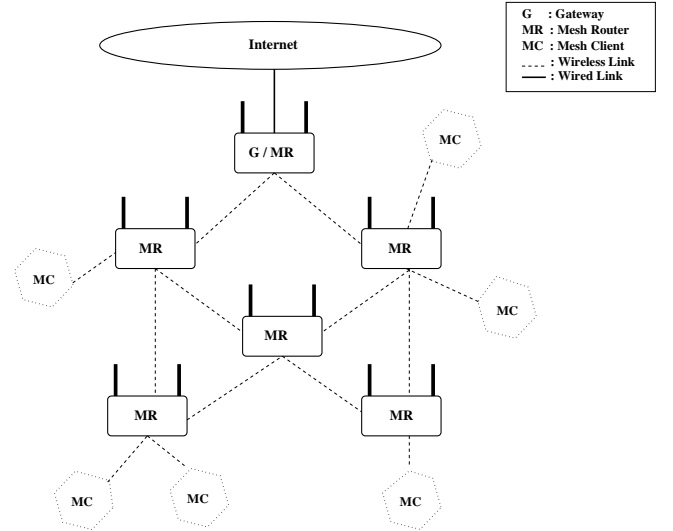


Fig. 1: A Simplistic WMN Architecture

IEEE 802.11 WMNs employing the multi-hop transmissions [8]. The most efficient and pervasive deployment architecture is the MRMC framework. Availability of non-overlapping channels under the IEEE 802.11 and IEEE 802.16 protocol standards, and cheap off-the-shelf wireless network interface cards, have propelled the application of MRMC WMNs. The IEEE 802.11b/g/n standard utilizes the unlicensed 2.4 GHz frequency band and provides 3 orthogonal channels centered at 25 MHz frequency spacing while the IEEE 802.11a/ac standard operates in the *unlicensed national information infrastructure* band (U-NII band) that ranges from 5.15 GHz to 5.85 GHz [9]. The assured number of orthogonal frequencies range from 12 to 24, depending upon the channel bandwidth *i.e.*, 20 or 40 MHz , and the country/region in context, as operation in some frequencies of the 5 GHz band may be restricted or may mandate the employment of some specific technologies as per local laws and policies. The presence of multiple radios on each node coupled with the availability of multiple channels, facilitates concurrent signal transmissions and receptions on the WMN nodes. Thus MRMC WMNs register an enhanced network capacity, increase in the bandwidth of the network and an improved spectrum efficiency [10] [11]. However, the technological enhancements in WMN

deployments have incidentally led to an undesired increase in the interference that impedes the radio communication in such wireless networks.

1.1. Research Problem Outline

Numerous research studies have attempted to address and resolve interference related issues in WMNs. But the notion of *Radio co-location Interference* or RCI *i.e.*, interference caused and experienced by spatially co-located radios or SCRs, that are operating on identical frequencies, is a crucial aspect of the multifaceted interference problem that has been largely unaddressed and finds very little mention in the current WMN research literature. We choose to focus primarily on this issue, and strive to adequately address and mitigate the adverse effects of RCI in a WMN. The first step towards mitigation of undesired detrimental affects of any interference bottleneck is its correct identification, and representation in the conflict graph. Thus, we accomplish our end goal by an accurate and wholesome representation of all possible RCI scenarios of a WMN in its *conflict graph*.

1.2. Paper Organization

In Section 2, we touch upon the important interference related themes such as categorization and representation of wireless interference and the *interference models*. In Section 3, we briefly mention and cite some notable research literature relevant to our study. Section 4 introduces the concept of RCI supplemented with two crucial RCI scenarios, and supports the theoretical arguments with an experimental *proof of concept*. In Section 5, we propose two generic multi-radio multi-channel conflict graph generation algorithms, *viz.*, a conventional approach and a novel radio co-location aware technique. Section 6 comprises of simulation methodologies and characteristics, presentation and analysis of recorded results, and a discussion on the reliability of total interference

degree as a theoretical estimate of prevalent interference. In Section 7, we derive concrete conclusions accompanied with certain logical inferences, predicated on the observed results and offered analysis. Finally, Section 8 outlines the future course of our research work.

2. INTERFERENCE IN WMNS

With the advent of MRMC deployments, the spectral complexity of the WMNs intensified. This led to a substantial rise in the interference endemic in WMNs, identification and mitigation of which continues to be the focus of researchers.

2.1. Categorizing Interference In A WMN

Interference in a WMN can be broadly classified into three categories *viz.*, external, internal and multipath fading [12]. In our work, we focus only on the internal or controlled interference, as it is the primary disruptive factor that leads to poor network performance in MRMC WMNs.

2.2. Interference Models

The next step would entail determining the conflicting wireless links in the WMN. This is a very complex problem due to the wireless nature of the network. Hence, researchers resort to employing a suitable and accurate network interference model for the WMN. The parameters of the model are used to ascertain the interfering or conflicting links. Selection of an appropriate model is not only crucial in representing complex wireless interference characteristics into a simple mathematical fashion, but also pivotal in studying the overall network performance and behavior, when subjected to the adverse effects of interference. The popular approaches taken to model the interference in wireless communication links are *the Physical or the Additive Interference Model*, *the Capture Threshold Model*, *the Interference Range Model* and *the Protocol Model* [13] [14].

2.3. Selection Of Interference Model

The Protocol Model is a simplified representation of physical interference which we use in our work for three reasons. It is a simple yet felicitous mathematical representation of the actual wireless interference. It permits a binary interference modeling, *i.e.*, a successful transmission is one which is not attenuated by any adjacent interfering signal active in its transmission range. Finally, there is no fixed interference range by which two communicating nodes need to be separated. Instead, the model gives us the flexibility of fixing the interference range as it is proportional to the distance between a communicating node pair.

2.4. Representing Interference In A WMN

Having successfully identified the interfering wireless links in a WMN, we need to represent these interference relationships. This representation is done by a special graph, called the *Conflict Graph*. Before we proceed, we state a few concepts and definitions. Let $G = (V, E)$ represent an arbitrary WMN.

- (a) **Potential Interference Link** : Let $i \in V, j \in V$, such that $(i, j) \in E$, then $\forall (m, n) \in E$, where the transmitting range of the radio at node m or n , extends upto, or beyond node i or j , are called the potential interference links of link (i, j) . They are also termed as conflicting links or contention edges.
- (b) **Potential Interference Number**: Let $i \in V, j \in V$, then the potential interference number of link $(i, j) \in E$, is the total number of links in E which are the potential interference links of (i, j) . It is also usually termed as *Interference Degree*.
- (c) **Total Interference Degree TID** : It is an approximate estimate of the adverse impact of the interference endemic in a WMN. It is arrived at by halving the sum of the *potential interference numbers* of all the links in the graph.

(d) **Conflict Graph (CG)** : $G_c = (V_c, E_c)$ is generated from graph $G = (V, E)$ where

- $V_c = E$ or $V_c = \{ (i, j) \in E \mid (i, j) \text{ is a wireless communication link} \}$
- $\{ ((i, j), (m, n)) \in E_c \mid (m, n) \text{ is a potential interference or conflict link of } (i, j) \text{ in } G \}$.

3. RELATED RESEARCH WORK

Interference substantially degrades the wireless network performance. It leads to low end-to-end throughputs and high transmission delays. Multi-hop transmissions in WMNs are adversely impacted by the co-channel interference, deteriorating network capacity and destabilizing fairness in link utilization [8]. effort to mitigate and restrain the impact of interference in WMNs. Conflict graphs serve as the primary indispensable tool for addressing the various WMN design and performance issues. They are extensively used for modeling and estimating the interference degree in wireless and cellular networks [15]. However, a basic conflict graph, or *CG*, is only suited to a wireless network in which each node is equipped with a single radio. In order to model the interference in an MRMC WMN, the concept of *CG* needs to be extended to an enhanced version called the *multi-radio multi-channel conflict graph* or an *MMCG*. Several research endeavors [4], [9], [15]–[24], directed at finding an efficient CA for an MRMC WMN have made use of the concept of MMCG to model the interference in their network scenario.

In [4], the authors merely suggest that the conflict graph was generated by ensuring that the *interference-to-communication* ratio is set to 2, with no further insight into the algorithmic aspects of this crucial step. In contrast, the literature in [16] defines in great detail, two approaches to generate conflict graphs. The first definition is centered on the *traffic flow interference*, employing the protocol model and assuming unidirectional traffic flows. The second approach takes into

account the *link interference* based on the extended protocol model. However, its evident that neither of the proposed techniques is inherently broad-based in its outlook. The former assumes a unidirectional traffic flow and mandates the application of the protocol model as the underlying interference model, while the latter necessitates the use of the extended protocol model, restricting both their approaches to specific WNN architectures. Likewise, authors in [9] define a conflict graph to be an undirected graph under the protocol model.

Authors in [17] provide a high level definition of CG, with an assurance that the concept is applicable to any interference model. However, they do not explicitly propose any algorithm. Further, they opine that a CG does not change with the assignment of channels to vertices. This is not a true characteristic of the MMCG of a WMN, as it may very well change when different *Channel Assignment* schemes are deployed in the WMN. Assignment of different channels to a link, under different CAs, alters the set of its conflict links, there by generating a different MMCG for each CA. Thus the authors' contention that a CG for a WMN will not change, does not hold true, atleast in the context of an MRMC deployment.

Authors in [18] discuss a single-channel CG and its multi-channel peer MMCG, for the protocol model, but without suggesting a methodical approach to generate either. In addition, they choose to map a link to a unidirectional flow and a bidirectional traffic is represented by two links. This underscores the fact that researchers tend to comprehend the interference dynamics, common to all WMNs, in a personalized myopic fashion, rather than adopting a broadly applicable view. In [19], the authors elaborate upon conflict graphs, with a special emphasis on *weighted* conflict graphs, for the protocol model. For the non-interfering or non-overlapping channels, they recommend that a CG be generated for each individual channel, and the overall CG for the WMN will be the union of all such single channel CGs. Thus they take a single-channel

view of an MRMC WMN, for multiple channels, and the final MMCG is an aggregate of the unique individual CGs. The approach is intuitive and simple, albeit for a medium to large scale WMN where each node is equipped with multiple identical NICs, and which leverages the availability of a high number of non-interfering channels, this fragmented view of a WMN to arrive at an MMCG will cause substantial implementation overhead.

The human perception of interference scenarios plays a significant role in the generation of a conflict graph. For example, the conflict relationship in a WMN demonstrated through an MMCG representation in [21] is quite different than that in [22]. The work in [21] aims to create a multi-dimensional CG by making use of a radio-link-channel tuple, while authors in [22] create a link-layer flow contention graph which is essentially a simple CG, that is based upon the number of channels allocated and the channel assignment to interfaces. Based on our review, we opine that the most generic and widely applicable of all MMCG creation procedures is suggested by *Ramachandran et. al.* [15]. The authors extend the conflict graph concept to model a multi-radio WMN, and generate a *multi-radio conflict graph* or an *MCG*. They describe the MCG generation approach stating explicitly that they employ an improvised vertex coloring algorithm to color the MCG, which ensures that each radio in the network is assigned a single channel. Yet, a lucid algorithm to generate the MCG is not proposed in the study. Any correlation between the MCG creation approach and the underlying interference model is not presented either. This leaves room for ambiguity while dealing with the question of dependence of the MCG creation technique upon the interference model being employed. Most importantly, the suggested approach and the corresponding illustration does not address the interference caused and experienced by SCRs operating on identical frequencies, and thus fails to represent the RCI scenarios in its interference estimate.

From the literature review presented above, we can conclude that the underlying fundamental concepts of a conflict link and a basic conflict graph, have been rightly employed by researchers in their work, but the creation of an MMCG in the research studies often depends upon one or more of the following factors.

- (a) The Interference Model being used, which is the *protocol model* in most studies.
- (b) The WMN Topology
- (c) Representation of Traffic Flows *i.e.*, unidirectional or bidirectional
- (d) Perception of the Interference scenarios

Further, we have not come across any research endeavor related to MMCG generation that adequately addresses or even highlights, the detrimental effect of multiple SCRs installed at a WMN node, that have been assigned the same channel to communicate on. In the upcoming sections we investigate and delve into the phenomena of RCI.

4. IMPACT OF SPATIAL CO-LOCATION OF RADIOS ON WMNS

An important aspect which most of the existing MMCG creation techniques fail to acknowledge, is the effect of spatial co-location of radios on wireless links, emanating from a node equipped with multiple radios. Such a node certainly stands to benefit if each one of its radios is assigned a different RF channel and can concurrently communicate with adjacent nodes, substantially raising the capacity of the node and the entire network. The surge in nodal throughput, and by virtue of aggregation, in the overall network throughput, can be tremendously accentuated if the RF channels being assigned are non-interfering or orthogonal. However, if two or more of such SCRs are operating on the same RF channel (or overlapping channels), not only is the multi-radio deployment rendered futile and its advantages negated, but is also adversely

impacted by the additional interference generated due to the spatial proximity of such SCRs. We restrict our study of this interference phenomena, to SCRs operating on the same channel, which is consistent with the binary interference model that we have adopted.

In this section, we investigate the impact of spatial co-location of radios on the overall interference scenario. We commence by elucidating two interference scenarios to elicit a theoretical proposition, and then experimentally validate the suggested argument.

4.1. Two Co-location Interference Scenarios

4.1.1. Case 1: Consider a trivial two node wireless network as illustrated in Figure 2. Node *A* is equipped with one NIC while node *C* is equipped with two identical NICs *i.e.*, a pair of identical SCRs. Nodes *A* and *C* are within each others transmission range and thus share a wireless communication link in the WMN.

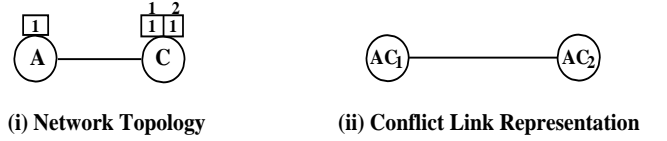


Fig. 2: Impact of spatially co-located radios

Since the wireless communication link between the nodes *A* and *C* is a RF transmission, by virtue of RF wave propagation, any transmission from node *A* will reach both radio C_1 and radio C_2 alike, as they are co-located at *C*. Similarly, both radio C_1 and radio C_2 are independently capable of a simultaneous transmission to the radio on node *A*. In the above scenario, by virtue of wireless propagation, it is perfectly logical to infer that links AC_1 and AC_2 are interfering links and ought to have an edge in the corresponding MMCG to denote their mutual interference.

4.1.2. Case 2: Consider the three flavors of a WMN layout depicted in the three cases of Figure 3. The nodes are equipped with one or more IEEE 802.11g radios, which are operating

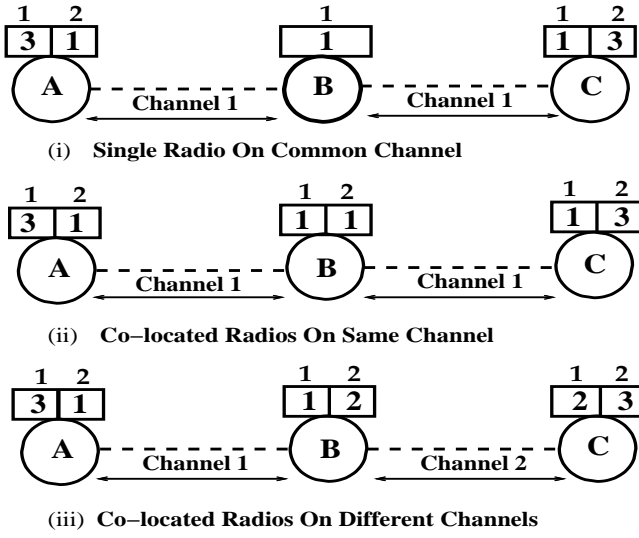


Fig. 3: Scenarios of radio co-location

on the radio frequencies explicitly illustrated. One of the three orthogonal channels 1, 2, & 3, as per the 802.11g specifications, are allocated to the radios. In Figure 3 (i), the extreme nodes, A and C , are equipped with a pair of SCRs each, while the node at the center, B , has a single radio. In Figure 3 (ii), all the three nodes are equipped with a pair of SCRs. Both the cases create a common-channel communication scenario, as is evident from the radio-channel allocations. There is, however, a fundamental difference which we deliberate over. With respect to node B , the former emulates a *Single-Radio* architecture, rejecting any possibility of RCI. In contrast, the latter has dual radios at node B , both assigned the same channel, and thus becomes the epicenter of RCI. The wireless links AB and BC in the depicted WMN layout are the potential conflicting links. Let us focus on node B and reiterate the argument presented in **Case 1** above. Thus, for the layout in Figure 3 (i), only the radio-link pairs A_2B_1 & C_1B_1 are conflicting links. But for the layout in Figure 3(ii), the total interference degree escalates substantially as there are six conflicting radio-link pairs, viz. A_2B_1 & A_2B_2 , A_2B_1 & B_1C_1 , A_2B_1 & B_2C_1 , A_2B_2 & B_1C_1 , B_2C_1 & B_1C_1 and A_2B_2 & B_2C_1 , all of which must rightfully share an edge in the corresponding MMCG to represent their

conflict. The WMN layout in Figure 3(iii) fully utilizes the inherent multi-radio multi-channel architecture, leading to an interference free deployment. Here, the wireless links AB and BC , represented by the radio-links A_2B_1 and B_2C_1 , have been assigned channels 1 and 2, respectively, and thus are non-conflicting.

Drawing from the stated theoretical arguments, we contend that the *Single Radio Common Channel* or *SRCC* operation in Figure 3 (i), will perform better than the *Multi Radio Common Channel* or *MRCC* operation in Figure 3 (ii), even if marginally so for such a trivial architecture. Further, the *Multi Radio Different Channel* or *MRDC* deployment in Figure 3 (iii), will significantly outperform the other two schemes.

4.2. Experimental Validation

To corroborate our argument with actual experimental data, simulations of the three network layouts illustrated in Figure 3 were performed in ns-3 [25].

4.2.1. Network Design: The inbuilt ns-3 TCP BulkSendApplication is employed to establish two TCP connections between node pairs A & B and B & C , for the cases (i), (ii), and (iii) of Figure 3, with the exact channel assignments to the corresponding radios. We install a TCP BulkSendApplication source each, at the nodes A & C . Both the TCP sinks are installed at node B , as it is the node common to all the conflicting links, and hence the focal point of maximum offered interference to the data communication. Each source sends a 10 MB data file to its corresponding sink. We observe and report the *Network Aggregate Throughput* for each of the three scenarios, which serves as a fair metric to gauge the adverse impact of interference in the WMN layout. Simulation parameters are listed in Table I.

4.2.2. Simulation Results: For each deployment, multiple independent sample runs were performed. We register the *Throughput* of only the onward flow, i.e., the *Source - Sink*

TABLE I: Co-location Experiment Simulation Parameters

Parameters	Values
Transmitted File Size	10 MB
Maximum 802.11 Phy Datarate	9 Mbps
RTS/CTS	Enabled
TCP Packet Size	1024 Bytes
Fragmentation Threshold	2200 Bytes
Inter-node Separation	250 mts
Propagation Loss Model	Range Propagation Loss Model

flow, for both TCP connections of each deployment, and illustrate the *Average Aggregate Network Throughput* recorded for the three scenarios, in Table II.

TABLE II: Co-location Experiment Simulation Results

Parameter	SRCC	MRCC	MRDC
Average Aggregate Network Throughput (Mbps)	3.19	3.01	5.87

The *SRCC* deployment performs slightly better than the *MRCC* deployment. This result vindicates our theoretical contention, that the surge in interference due to SCRs, operating on a common channel, degrades the network performance substantially. As can be inferred from the results in Table II, it is very likely that the corresponding *SRCC* deployment may fare better. Here, the difference in the *Average Network Aggregate Throughput* of the two deployments is less than 10%, which is not remarkable. However, we ought to appreciate the notion that in medium to large *MRMC* WMNs, the presence of SCRs which have been assigned the same channel, in moderate to large numbers, will in all likelihood exacerbate the adverse effects of this additional RCI. It is thus imperative that we take cognizance of the RCI phenomena, and address its adverse impact on the performance of a WMN. The first step of this exercise would be to appropriately represent the co-location-interference in the interference model of a WMN. The *Multi-Radio Different-Channel* or the *MRDC* deployment offers an *Aggregate Network Throughput*, that is almost twice that of a trivial *SRCC* deployment. This is in conformity with

our theoretical supposition as well. We can safely conclude, that the results of this investigation substantiate the proposed theoretical concept of RCI *i.e.*, the *interference caused by SCRs* which have been assigned a common-channel.

But representation of the RCI is lacking in the MMCG creation method suggested in [15], and all other research work focussed on minimization of interference in WMNs that we referred to. The underlying reason is that while creating the MMCG, the fact that multiple radios installed on the same node are spatially co-located is not accounted for. A result of this oversight is that a few interference scenarios escape notice during the MMCG creation and the estimate is seldom a true reflection of the actual interference scenario in the network. Having laid the theoretical foundations, supplemented with experimental evidence, we formally state the research problem we aim to pursue and address, in the next sub-section.

4.3. Problem Definition

Multi-Radio Multi-Channel conflict Graphs or *MMCGs* are frequently used to accurately represent the interference present in a WMN and measure its intensity or degree of impact on the WMN. Thus, a generic approach to create an MMCG for any arbitrary WMN is of utmost importance. The need for a comprehensive procedure to generate an MMCG $G_c = (V_c, E_c)$ for a given input WMN graph $G = (V, E)$, which is independent of the factors such as the *WMN topology*, the *choice of interference model*, the *channel allocation* scheme etc., is often felt by researchers attempting to solve CA, routing or maximum-throughput problems in a WMN.

To the best of our knowledge, a lucid, all-encompassing and explicitly proposed algorithm for MMCG creation, especially one which factors in the effects of SCRs, is lacking in the current research literature. The novel concept, of the phenomena of RCI, and the redressal of its adverse impact on the performance of a WMN by adequate and accurate representation

in the creation of its MMCG, is what distinguishes our study from the plethora of approaches suggested before.

5. THE PROPOSED MMCG GENERATION ALGORITHMS

To remedy the lack of a broad-based algorithm, we now propose two generic polynomial time algorithms to create a multi-radio multi-channel conflict graph or an *MMCG*. We designed the algorithms with the vision of creating a generic, widely applicable and versatile method of generating MMCGs. We have tailored the algorithms in conformity with our broad-based approach, and ensured their structural and functional independence from the commonly encountered constraints listed below.

- (a) ***The Choice of Interference Model***: As stated earlier, we employ the protocol interference model to determine the interfering links. This however, is not binding upon the algorithms, and any interference model can be chosen in its stead. The algorithms allow the underlying interference model to define a conflicting link. Thus the choice of the interference model is not an implementation constraint.
- (b) ***WMN Topology***: The algorithms are topology independent and applicable to all WMN deployments. The graphical representation, however, must be a connected graph. This condition is reasonable, necessary and not an impediment, as having an isolated node with no wireless connectivity to any other node in the WMN is wasteful.
- (c) ***Number of Radios and Channels*** : The algorithms are also applicable to both single channel and multi-channel WMN deployments *i.e.*, they can create MMCGs for the same WMN topology for both, a common CA and a varying/multiple CA.
- (d) ***The Channel Assignment or CA Scheme*** : The algorithms not only generate an initial *multi-radio conflict graph*, whose edges denote potentially interfering links when every radio is assigned the same channel, but

they can as easily generate a *multi-radio multi-channel conflict graph* or an MMCG, which depicts the actual state of interference in a WMN deployment in which a CA scheme is implemented. The output MMCGs will certainly differ if the CA scheme in the network changes.

- (e) ***Interpretations of Interference Scenarios***: The algorithms, especially the one which takes into account the radio co-location factor, consider every possible interference scenario in the WMN, thereby avoiding the variations associated with varying human interpretations of interference scenarios.

The first algorithm we propose, does not take into account the effect of spatial co-location of multiple radios on a node. It follows a conventional approach, variations of which have been employed in various research endeavors, customized to suit the model being implemented. However, a generic algorithm, independent of the aforementioned constraints has not been formally proposed, a void we intend to fill. We christen it *The Classical MMCG* algorithm, or *C-MMCG*. The second algorithm effectively factors the RCI into its interference modeling logic. It paints a more comprehensive and wholesome picture of the interference scenario in the given WMN, and is thus a notable improvement over *C-MMCG*. We name it *The Enhanced MMCG* algorithm, or *E-MMCG* for the ease of reference. The two broad scenarios in a WMN where the proposed MMCG algorithms find great utility are elucidated below.

- (a) ***Prior to CA*** : Before the CA exercise is carried out in a WMN, usually all the radios are initially assigned a default channel. The MMCG resulting from this default channel configuration represents a maximal prevalent interference scenario and thus serves as an ideal input to a CA algorithm.
- (b) ***After CA*** : After the radios have been assigned appropriate channels in accordance with the applied CA scheme,

the proposed MMCG algorithms may be used to generate the TID estimate for the WMN. This desirable feature facilitates a theoretical assessment of the efficacy of the CA approach employed.

Now we propose the two algorithms along with their functional description.

Algorithm 1 C-MMCG : Radio Co-location Not Considered

Input: $G = (V, E)$, $R_i(i \in V)$, $N_i(i \in V) = \{ j | (j \in V) \&\& (i \neq j) \&\& ((i, j) \in E) \}$
Initially : $V' \leftarrow \emptyset$, $E' \leftarrow \emptyset$, $V_c \leftarrow \emptyset$, $E_c \leftarrow \emptyset$
Notations : $G \leftarrow$ WMN Graph, $R_i \leftarrow$ Radio-Set, $N_i \leftarrow$ Neighbour Set
Output: $G_c = (V_c, E_c)$

```

1: for  $i \in V$  do
2:    $V' \leftarrow V' + R_i$ 
3:   for  $j \in N_i$  do
4:     for  $x \in R_i, y \in R_j$  do
5:       for  $y \in R_j$  do
6:          $E' \leftarrow E' + (x, y)$ 
7:       end for
8:     end for
9:   end for
10: end for {Get the intermediate graph  $G' = (V', E')$ }
11: for  $(i, j) \in E$  where  $i \in V, j \in V$  do
12:    $V_c \leftarrow V_c + (i, j)$ 
13: end for {Create the Vertex Set  $V_c$  of the CG  $G_c$ }
14: for  $v \in V_c, u \in V_c, v \neq u$  do
15:   Use an Interference Model to determine if  $u$  &  $v$  are Potentially Interfering Links
16:   if True then
17:     if  $Channel(u) == Channel(v)$  then
18:        $E_c \leftarrow E_c + (u, v)$  {Create the Edge Set  $E_c$  of the CG  $G_c$ }
19:     end if
20:   end if
21: end for {Output C-MMCG  $G_c = (V_c, E_c)$ }
```

5.1. The Classical MMCG Algorithm

The *C-MMCG* algorithm adopts a conventional approach to model the interference endemic in WMNs. Its stepwise procedure is described in Algorithm 1. Steps 1 to 10 split each node in the original WMN topology graph $G = (V, E)$, into the number of radios it is equipped with, and generate an intermediate graph $G' = (V', E')$, where V' represents the

set of total number of wireless radios in the WMN and E is edge set of links between radio pairs.

While G reflects a node centric view of the WMN, G' reflects the view of the WMN at the granularity of individual radios. Step 2 splits the radio set of each node in G to individual radio-nodes in G' . Steps 3 to 10, process the neighbor set of a node in G , to create edges in E' , for each individual radio in the radio-set of the node in context. The intermediate graph G' becomes the input for the final MMCG creation step. In steps 11 to 13, the vertex set V_c of the MMCG is populated by adding elements of the edge-set E' . Further, in steps 14 to 21, the vertices in V_c are processed pairwise, and a corresponding edge is added to the MMCG edge-set E_c , iff the vertex pair being currently processed is conflicting, and both the vertices have been assigned the same channel. The function *Channel()* fetches the channel assigned to a particular vertex of G_c . As described earlier, the channel returned by the function would be the default channel if the algorithm is being applied to a WMN prior to the CA exercise. Else, *Channel()* would fetch the channel that has been assigned by the CA scheme employed in the WMN. Whether a vertex pair is conflicting, is determined by the underlying interference model. We have employed the *Protocol Interference Model* and as stated earlier, any other interference model may be used as well. Algorithm 1 finally outputs the *C-MMCG*, G_c . The algorithmic time complexity is $O(n^2)$, as each of the three functional steps viz., creating the intermediate graph G' , generating the vertices of C-MMCG G_c , and finally adding the edge set to C-MMCG G_c , have an $O(n^2)$ computational complexity, where n is the number of nodes in the WMN.

5.2. The Enhanced MMCG Algorithm

The *E-MMCG* considers all possible interference scenarios that exist in a WMN, including the RCI. The stepwise procedure to generate an E-MMCG for a WMN is described in

Algorithm 2. In addition to the *C-MMCG* logic, Algorithm 2 also captures interference due to spatial co-location of radios in the WMN. In steps 22 to 28, the algorithm adds an edge between two vertices of the E-MMCG, **iff**

- (a) The corresponding pair of wireless links in the WMN originate or terminate at the same node and,
- (b) The links have been assigned the same channel.

Algorithm 2 E-MMCG : Radio Co-location Considered

Input: $G = (V, E)$, $R_i (i \in V)$, $N_i (i \in V) = \{ j | (j \in V) \&\& (i \neq j) \&\& ((i, j) \in E) \}$

Initially: $V' \leftarrow \emptyset$, $E' \leftarrow \emptyset$, $V_c \leftarrow \emptyset$, $E_c \leftarrow \emptyset$

Notations: $G \leftarrow$ WMN Graph, $R_i \leftarrow$ Radio-Set, $N_i \leftarrow$ Neighbour Set

Output: $G_c = (V_c, E_c)$

```

1: for  $i \in V$  do
2:    $V' \leftarrow V' + R_i$ 
3:   for  $j \in N_i$  do
4:     for  $x \in R_i, y \in R_j$  do
5:       for  $y \in R_j$  do
6:          $E' \leftarrow E' + (x, y)$ 
7:       end for
8:     end for
9:   end for
10: end for {Get the intermeditate graph  $G' = (V', E')$ }
11: for  $(i, j) \in E$  where  $i \in V, j \in V$  do
12:    $V_c \leftarrow V_c + (i, j)$ 
13: end for {Create the Vertex Set  $V_c$  of the  $CG G_c$ }
14: for  $v \in V_c, u \in V_c, v \neq u$  do
15:   Use an Interference Model to determine if  $u \& v$  are
   Potentially Interfering Links
16:   if True then
17:     if  $(Channel(u) == Channel(v))$  then
18:        $E_c \leftarrow E_c + (u, v)$  {Create the Edge Set  $E_c$  of the
        $CG G_c$ }
19:     end if
20:   end if
21: end for
22: for  $v \in V_c, u \in V_c, v \neq u ; v = (a, b), u = (c, d) ;$ 
    $a, b, c, d \in V$  do
23:   for  $i \in V$  do
24:     if  $[(a \in R_i \& b \in R_i) \&\& (c \in R_i \& d \in R_i)] \&\&$ 
      (Both elements of  $R_i$  on same channel) then
25:        $E_c \leftarrow E_c + (u, v)$  {Output E-MMCG  $G_c =$ 
       $(V_c, E_c)$ }
26:     end if
27:   end for
28: end for

```

The RCI accounting steps will apply to both common and multiple channel deployments in the WMN, preserving its generic nature. E-MMCG thus ensures that the interference scenarios discussed in Section 4, which are not being addressed in the existing research literature are accounted for, and the injection of the RCI into the overall interference dynamics is duly represented, by addition of necessary and sufficient links in the E-MMCG. The links added to the E-MMCG to account for the RCI, are characteristic of the E-MMCG algorithm, and to be more precise, are generated from its steps 22 to 28. These conflicting links may or may not be determined by the employed interference model, but they most certainly will not escape notice of the E-MMCG algorithm. The time complexity of the algorithm, similar to its conventional counterpart C-MMCG is $O(n^2)$.

5.3. C-MMCG and E-MMCG : An Illustration

Let us pictorially demonstrate, through Figure 4, the output MMCGs for the two flavors proposed above. Figure 4 (i) depicts the original WMN topology, which consists of four nodes, A, B, C and D , where each is assigned 2, 1, 1, and 2 number of radios, respectively. Each radio is operating on the default channel, so the two methods will generate the initial, maximal-conflict MMCG for the WMN. The graphical representations of C-MMCG and E-MMCG, for the given WMN layout, are exhibited in cases (ii) and (iii) of Figure 4, respectively. Upon observation, it is evident that E-MMCG has all the conflicting links present in C-MMCG, and in addition contains four more interfering links, viz. $A_0B_0 - A_1C_0$, $A_1B_0 - A_0C_0$, $B_0D_0 - C_0D_1$ and $C_0D_0 - B_0D_1$. These four conflicting links are the offspring of the RCI, caused by the wireless transmissions from radios spatially co-located at nodes A and D .

The number of these additional conflict links caused by RCI increases drastically with the size of the WMN, which we

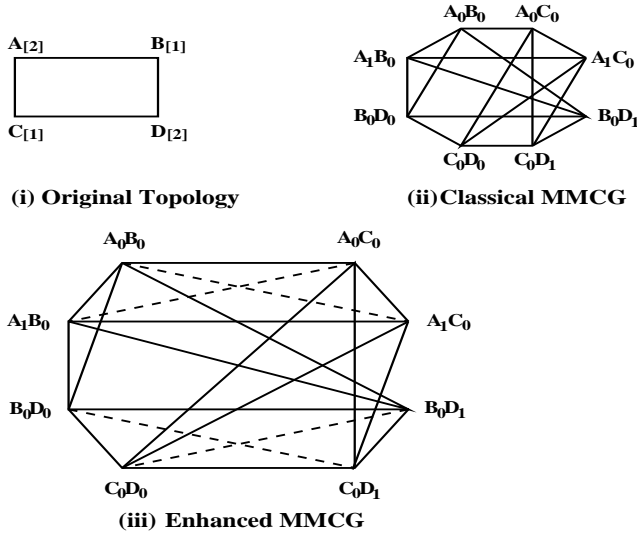


Fig. 4: An illustration of Classical and Enhanced MMCGs for a given Topology

demonstrate in Section 6. The ability of E-MMCG algorithm to capture and represent the interference scenarios spawned by RCI is the first step towards alleviating the adverse impact of RCI.

6. SIMULATIONS, RESULTS AND ANALYSIS

Having proposed the MMCG algorithms, especially the one based on the concept of co-location of radios, it is imperative we prove their relevance in real-world WMN deployments. We take a three pronged approach in this regard.

6.1. Measuring Impact Of Interference

We employ the MMCG algorithms to measure the *TID* in a WMN, and compare the results of the two flavors. We consider a square *Grid Layout* for the WMNs, of size $5n \times 5n$ where $n = \{1, 2, \dots, 10\}$, thus varying the size of WMNs from 5×5 nodes to 50×50 nodes, where all the nodes are equipped with 2 identical radios, and all radios are on a *common channel*. This configuration represents a *maximum interference* scenario, and is ideal for analysis. We apply both MMCG algorithms to each of these grid topologies. The results are illustrated in Figure 5. The statistics in Figure 5 elicit the fact that E-MMCG which considers co-location of radios, accounts for all the

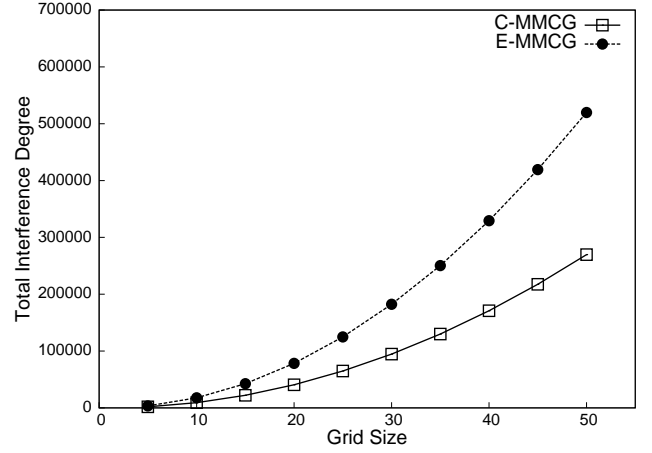


Fig. 5: TID Comparison of C-MMCG vs E-MMCG

potential interfering links or *interference scenarios* present in a WMN, and thus registers substantially high values of *TID*. C-MMCG, however, suffers from limited potency to probe a WMN for *potential interfering links* as it does not factor in the ramifications of the presence of SCRs on a common channel. This is reflected by its poor accounting of *Interference Degree* values as compared to its enhanced counterpart, E-MMCG. Further, as the size of WMN grows, the difference in the *TID* of the two MMCG approaches becomes increasingly prominent. This implies that there is a tremendous upsurge in the RCI as the size and complexity of the WMN increases. This finding further consolidates the proposition we put forward in Section 4, that the adverse impact of RCI gets more pronounced in medium to large WMNs, must be appropriately accounted for, and adequately addressed.

6.2. Application to CA Algorithms

Since *Conflict Graphs* serve as the input to *Channel Assignment* algorithms, the next logical step is to apply the MMCG algorithms to two graph-theoretic solutions of the CA problem. In [22] authors propose a *Breadth First Search* approach or BFS-CA, which is a centralized dynamic algorithm that employs the services of a *channel assignment server* or CAS. Initially, the WMN is assigned a default channel that experiences the least interference from intentional or un-intentional

interferers in close proximity, based on a channel-ranking technique. The CAS computes the average distance of each vertex in the multi-radio conflict graph, or the MCG, from the gateway. Thereafter, the algorithm performs a breadth-first scan of the MCG, starting from the vertices closest to the gateway, assigning a channel to each vertex that it encounters, which is orthogonal to the channels assigned to its neighbors if possible. Else, it selects a channel randomly from the set of available channels and allots it to the vertex in context. A *Maximal Independent Set* channel assignment scheme or MaIS-CA is proposed in [24]. It is a greedy heuristic scheme, which determines the maximal independent set of vertices in a conflict graph, assigns them an identical channel and then removes them from the conflict graph. This process is iterated, until all the vertices have been assigned a channel.

We opine that MaIS-CA is algorithmically superior than BFS-CA, as its CA approach distributes the channels among the radios in a more balanced fashion, and also assures a higher degree of connectivity in the WMN graph. For a theoretical validation of the stated notion, we implement these two CA algorithms over Grid WMNs using both C-MMCG and E-MMCG as the input to CA schemes, and then estimate the *TID* for each CA deployment. The nodes are equipped with 2 identical radios each, and we utilize the 3 non-overlapping channels guaranteed by IEEE 802.11g specifications. For a smooth discourse hereon, we adopt the following nomenclature to differentiate between the CAs.

- *C-MMCG based CAs* : BFS-CA₁ and MaIS-CA₁.
- *E-MMCG based CAs* : BFS-CA₂ and MaIS-CA₂.

The procedure we follow is described below :

- Take WMN grid of size $n \times n$, where $n \in \{3, 5, 10\}$.
- Create two *MMCGs* using the algorithms C-MMCG and E-MMCG.
- Use both flavors of MMCG as input to BFS-CA and MaIS-CA to obtain final CAs, 4 in all.

- Apply C-MMCG on BFS-CA₁ & MaIS-CA₁ and E-MMCG on BFS-CA₂ & MaIS-CA₂, to estimate their respective *TIDs*.

This procedure will furnish the theoretical measure of impact of interference in each of the final CAs. We subject a particular version of CA to its corresponding MMCG version for the *TID* estimate for consistency. Further, we only compare two CAs generated from the same MMCG approach. Comparing the interference estimate of a C-MMCG CA with an E-MMCG CA is not logical, because the approaches to generate these estimates are not identical.

TABLE III: A Comparison of *TIDs* of the MMCG CAs

Grid Size	TID			
	BFS-CA		MaIS	
	C-MMCG	E-MMCG	C-MMCG	E-MMCG
3×3	82	70	16	56
5×5	436	716	142	488
10×10	2098	2470	834	2036

It can be inferred from Table III, that the BFS-CA of a particular MMCG version registers a higher measure of interference than the corresponding MaIS-CA, *i.e.*, with respect to *TID* of CAs, $BFS-CA_1 > MaIS-CA_1$ and $BFS-CA_2 > MaIS-CA_2$. This result strengthens the argument that MaIS-CA is a better CA scheme than BFS-CA, and our simulation results will, in all likelihood, conform to the pattern. Further, it assures us theoretically that employing the use of E-MMCG approach does not alter the intrinsic algorithmic disposition of a CA.

6.3. Simulation Testbed For Performance Evaluation Of CAs

The final step in this research investigation entails that we monitor and analyze the performance of the BFS-CA and MaIS-CA, for both versions of the MMCG, through simulations. We create an extensive data traffic scenario by considering various single-hop and multi-hop transmission combinations. Our objectives are four fold.

- (a) To compare the performance characteristics of E-MMCG

CA against that of the C-MMCG version, for the same CA algorithm.

- (b) To compare the performance of the two approaches, BFS-CA and MaIS-CA, for both versions of MMCG.
- (c) To observe the relative difference between the performances of BFS-CA and MaIS-CA, in the two versions of MMCG.
- (d) To observe the traffic interruptions or abrupt flow terminations, for a CA, in both versions of MMCG.

Through objectives (b) and (c) above, we intend to study the behavior of CAs for consistency in performance *i.e.*, if $X-CA$ performs better than $Y-CA$ in C-MMCG, then we opine that it should outperform $Y-CA$ in the E-MMCG model as well. Further, we also study the difference between the performance of $X-CA$ and $Y-CA$ in the two scenarios, for a relative comparison.

6.3.1. Simulation Design Parameters: We consider a 5×5 grid WMN, which provides some semblance of a large-scale topology. Since we intend to gauge the impact of interference on the WMN, we choose the *Aggregate Throughput* of the network, as the primary performance metric to be monitored. The total capacity of a network consistently degrades with the increase in interference, and it is thus a suitable and sufficient metric. We also employ *Average Packet Loss Ratio* as a metric for some scenarios since it is also an ideal indicator of the disruption caused by prevalent interference to data transmission. Thus, TCP and UDP are the underlying transport layer protocols we have chosen for the experiments. The inbuilt ns-3 models of *BulkSendApplication* and *Udp-ClientServer* are leveraged for TCP and UDP implementations, respectively. TCP simulations are aimed at estimating the *Aggregate Network Throughput* while the UDP simulations are employed to determine the *Average Packet Loss Ratio* (PLR) and the *Mean Delay* (MD).

The radios installed on all nodes are identical IEEE 802.11g

radios, operating in the standard specified 2.4 GHz spectrum, which allows them to have up to 14 channels at their disposal, of which 3 channels are orthogonal. We restrict the number of available channels to these 3 non-interfering channels. We employ the *ERP-OFDM* modulation technique, with a ceiling of 9 Mbps on the maximum PHY data-rate. We let the transmission power assume the default value of 16.02 dBm, and set the receiver gain to -10 dBm for better sensitivity. Nodes are placed at a separation of 200 mts, so that the adjacent nodes lie comfortably within the transmission range of the node in context. Use of *Range Propagation Loss Model* in ns-3 facilitates an easy implementation of the *protocol model* for interference modeling. The simulation parameters are listed in the Table IV.

TABLE IV: ns-3 Simulation Parameters

Parameters	Values
Grid Size	5×5
No. of Radios/Node	2
Range Of Radios	250 mts
Available Orthogonal Channels	3
Maximum 802.11 PHY Datarate	9 Mbps
Maximum Segment Size (TCP)	1 KB
Packet Size (UDP)	1KB
Fragmentation Threshold	2200 Bytes
RTS/CTS(TCP)	Enabled
RTS/CTS(UDP)	Disabled
Routing Protocol Used	OLSR
Loss Model	Range Propagation
Propagation Model	Constant Speed

6.3.2. Data Traffic Characteristics: The most critical step in studying the impact of interference in a WMN is to tailor the right set of traffic flows, which will identify and expose the interference bottlenecks. To simulate a data traffic with suitable characteristics, we consider five types of TCP/UDP traffic flows which include both, single and multi-hop flows, and deploy a combination of these flow-types to characterize the intensity of interference present in a 5×5 grid WMN.

The 25 nodes in the WMN grid are numbered from 1 to 25, for the sake of representation. The traffic flows are depicted in Figure 6, followed by a brief description of each flow. The TCP/UDP client or *source*, can be identified by the dotted tail of the link representing the TCP/UDP connection, while the arrow-head signifies the TCP/UDP server or the *sink*.

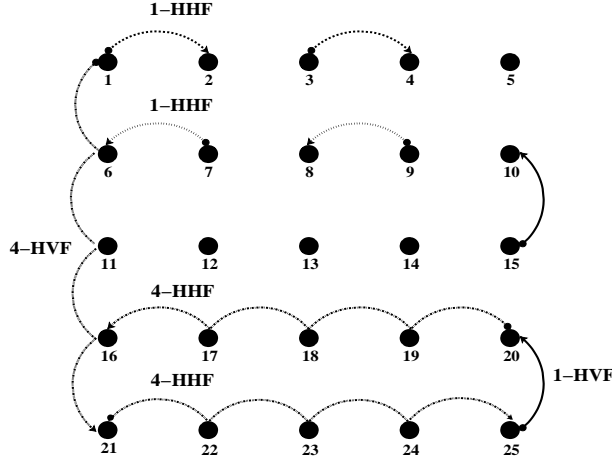


Fig. 6: Grid Layout

- (a) *One Hop Horizontal Flow or 1-HHF* : Single Hop TCP connections are established between alternate node pairs in all the rows of the WMN grid depicted in Figure 6. For example, in row 1, node-pairs (1 & 2) and (3 & 4) have a one hop TCP connection. TCP source application is installed on the node represented by a smaller number, and the sink application on the node bearing the bigger number in the node-pair.
- (b) *One Hop Vertical Flow or 1-HVF* : In addition to the 1-hop horizontal flows, one hop TCP vertical flows, between alternate node-pairs in each column in the bottom-up direction, are also generated.
- (c) *Four Hop Horizontal Flow or 4-HHF* : Since multi-hop transmission is an inherent trait of WMNs, we deploy TCP/UDP connections between the first and last nodes of each row, which are four hops away, to capture the interference characteristics of this trait.
- (d) *Four Hop Vertical Flow or 4-HVF* : To capture the spatial

interference characteristics of the grid in the vertical direction, TCP/UDP connections are established in a top-down fashion *i.e.*, between the first and last nodes of each column, which are four hops away.

- (e) *Eight Hop Diagonal Flows or 8-HDF* : The diagonally opposite node-pairs (1 & 25) and (21 & 5) have a TCP/UDP connection each, and generate eight-hop TCP/UDP flows, which is the maximum number of hops between a source and destination pair, in the given simulation grid test-bed.

6.3.3. Simulation Terminology, Scenarios and Statistics: To keep the discourse lucid and coherent, we first define some terms we use in the upcoming sections, specifically in the context of the simulations we run.

- (a) *Flow* : It refers, precisely, to the onward TCP/UDP traffic flow from a TCP/UDP source to the TCP/UDP sink.
- (b) *Abrupt Flow* : In all the TCP connections, we mandate that the source transmit *10 MB* data to the sink. For a TCP connection to be deemed successful, it is imperative that the sink receive the *10 MB* data sent by the source in entirety. Else, the TCP connection is considered to have abruptly terminated, and the flow to be an *Abrupt Flow*. Abrupt flows are a measure of the obstructions caused by prevalent interference to the data transmissions in a WMN. This notion is predicated on the fact that routing failures are often caused by high levels of interference in multi-hop wireless networks [26]. Loss of routing information causes packets buffered at intermediate relay nodes to be dropped. Since the routing protocol is singularly responsible for the routing mechanism, a TCP source may never be aware of an alternate route or route re-establishment. Thus, after subsequent failed attempts at re-transmitting the packets, a connection-timeout is invoked at the source and eventually the flow is abruptly terminated.

- (c) *Abrupt Flow Count* : The sum of the number of Abrupt Flows encountered, in all the simulations of a *Test Case Class*, for a CA.
- (d) *Throughput* : It refers to the *Average Network Aggregate Throughput*, which is the aggregate throughput of all the flows in a simulation, averaged over all such identical simulations that were run.
- (e) *Flow-RX* : A 4-HHF TCP flow in any row X of the grid.
- (f) *Flow Type-Y or FT-Y* : A set of all possible combinations of 4-HHFs taken Y at a time, where $Y \in \{1...5\}$. Thus, FT-1 would be a set containing 5C_1 or five 4-HHFs, viz. Flow-R1, Flow-R2, Flow-R3, Flow-R4 and Flow-R5.

We segregate the simulation scenarios into combinations of one-hop flows and multi-hop flows. The underlying motivation is to monitor the behavior of CAs for single-hop flows, and more complex multi-hop flows, separately. The test cases have been categorized into the following three classes.

(a) Test Case Class 1 : Flow Sustenance Testing

In the test cases belonging to this class, numerous one-hop TCP connections are concurrently active. The motivation here is to highlight the capability of a WMN to establish and sustain multiple TCP connections, under the debilitating effects of the endemic interference. Thus, these test cases are focused on the number of abrupt flows encountered, rather than the throughput. The test cases under this class are listed below.

- (i) *Test Case 1* : Only vertical flows i.e., 1-HVFs.
- (ii) *Test Case 2* : Only horizontal flows i.e., 1-HHFs.
- (iii) *Test Case 3* : All vertical and horizontal flows i.e., 1-HVFs + 1-HHFs.

(b) Test Case Class 2 : Flow Injection Testing

Multi-hop transmissions are a primary characteristic of WMNs. Concurrent multi-hop data connections are also the perfect instruments for estimating the adverse impact

of interference on the network capacity, as they transmit in tandem, triggering and intensifying the intricate interference bottlenecks in a WMN. We start with a single 4-HHF, and then inject one additional 4-HHF in each subsequent test-case. We monitor the network response to injection of fresh four-hop flows, and obtain a reliable estimate of the network capacity or the throughput for a variety of combinations of 4-HHFs. Here we focus on monitoring the throughput response of the network and not the number of abrupt flow terminations.

The goal here is to record the variation in network performance with the continuous injection of additional four-hop flows, hence it will suffice to do so for flows along the rows of the grid. We consider the five 4-HHFs i.e., Flow-R1...Flow-R5, and create a test-case for each *Flow Type-Y* or *FT-Y*, where $Y \in \{1...5\}$. Thus, we have the following test cases.

- (i) *Test Case 1* : FT-1 i.e., 5C_1 4-HHF combinations.
- (ii) *Test Case 2* : FT-2 i.e., 5C_2 4-HHF combinations.
- (iii) *Test Case 3* : FT-3 i.e., 5C_3 4-HHF combinations.
- (iv) *Test Case 4* : FT-4 i.e., 5C_4 4-HHF combinations.
- (v) *Test Case 5* : FT-5 i.e., 5C_5 4-HHF combinations.

(c) Test Case Class 3 : Load or Stress Testing

A reliable measure of network performance is often gauged under peak load, as it exhibits a network's resilience to bottlenecks that occur only at high traffic demands. We perform four test cases of increasing data traffic demands, and by virtue of the corresponding rise in the number of radio transmissions, of increasing interference complexities in the network. For each of these scenarios, we observe and analyze not only the network capacity, but also the packet loss ratio (PLR) and mean delay (MD). Thus both TCP and UDP simulations are run for the test-cases described below.

- (i) *Test Case 1* : D2 *i.e.*, Concurrent twin diagonal TCP/UDP flows or 8-HDFs.
- (ii) *Test Case 2* : H4V4 *i.e.*, Eight Concurrent TCP/UDP flows comprising of adjacent 4-HHF and 4-HVFs, each taken four at a time. A total of four such combinations, for which simulations are run and the average throughput is considered.
- (iii) *Test Case 3* : H5V5 *i.e.*, Ten concurrent TCP/UDP flows consisting of all five 4-HHFs and all five 4-HVFs.
- (iv) *Test Case 4* : H5V5D2 *i.e.*, Twelve concurrent TCP/UDP flows consisting of all five 4-HHFs, all five 4-HVFs, and both 8-HDFs.

6.4. Results and Analysis

The four CAs, BFS-CA and MaIS-CA for both versions of MMCG, are subjected to all the test-cases listed above. The metrics we monitor, and register for subsequent analysis are, the *Average Network Aggregate Throughput* which we will simply refer to as the *Throughput*, the *Abrupt Flow Count*, the *Packet Loss Ratio* and the *Mean Delay*.

TABLE V: Test Case Class 1 Results - Throughput

Average Network Aggregate Throughput (Mbps)			
BFS-CA		MaIS	
Test Case 1 → 1-HVFs			
<i>BFS-CA</i> ₁	<i>BFS-CA</i> ₂	<i>MaIS-CA</i> ₁	<i>MaIS-CA</i> ₂
16.73	18.40	24.31	24.44
Test Case 2 → 1-HHFs			
<i>BFS-CA</i> ₁	<i>BFS-CA</i> ₂	<i>MaIS-CA</i> ₁	<i>MaIS-CA</i> ₂
19.05	20.41	21.95	19.55
Test Case 3 → 1-HVFs + 1-HHFs			
<i>BFS-CA</i> ₁	<i>BFS-CA</i> ₂	<i>MaIS-CA</i> ₁	<i>MaIS-CA</i> ₂
24.99	25.36	32.35	34.16

6.4.1. Test Case Class 1:

We now present the recorded results, and methodically analyze them in adherence to the four objectives stated in sub-section C. the WMN, leave the possibility of localized pockets of

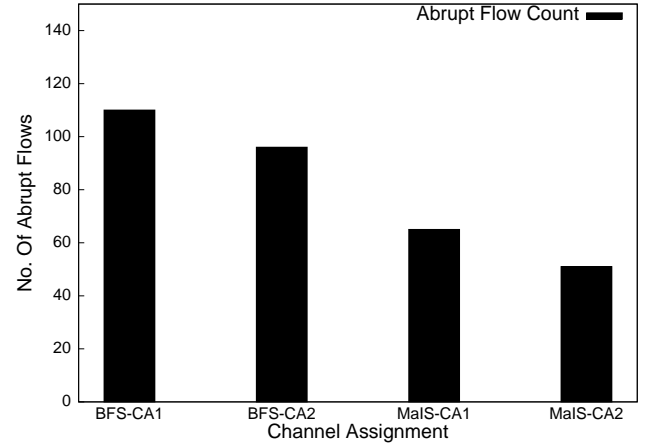


Fig. 7: Abrupt Flow Count in Test Case Class 1

high interference in the WMNs. Here, MaIS-CA₂ creates a slightly more intense *interference zone* than MaIS-CA₁, when throughput metrics of forward horizontal one-hop TCP flows are impinged by the interference offered by the reverse one-hop flows. This exception is reversed in the *Test Case 3*, *i.e.*, All 1-HHFs and 1-HVFs, which is a more comprehensive test scenario, and a relatively better case for observing throughput as a metric.

The metric of relevance here is the *Abrupt Flow Count*, which for C-MMCG CAs is quite higher than the corresponding E-MMCG CAs. This can be inferred from the graph displayed in Figure 7. We are able to achieve a 12.7% reduction in abrupt termination of flows over BFS-CA₁, in BFS-CA₂ simulations. Likewise, in MaIS-CA₂, we record a 21.53% drop in Abrupt Flow Count, when compared to MaIS-CA₁. Further, a comparison of the two CA approaches underscores the consistency of MaIS-CA outperforming BFS-CA, in both the MMCG approaches. In terms of Abrupt Flow Count, MaIS-CA₁ registers 40.9% lesser abrupt flow terminations than BFS-CA₁, and this improvement is more accentuated in MaIS-CA₂ where the frequency of abrupt flows depreciates by 46.8% when compared to BFS-CA₂.

A view from the vantage point of relative performance, will highlight the fact that in terms of Abrupt Flow Count, E-

MMCG approach further heightens the edge that MaIS-CA has over BFS-CA. This is evident from the *relative decrease* of 14.4% in the number of abrupt flow terminations achieved in the E-MMCG CAs, over their C-MMCG peers. This result is arrived at by the simple expression ($\% \text{ Drop in E-MMCG} - \% \text{ Drop in C-MMCG} / \% \text{ Drop in C-MMCG}$).

Although not of great relevance here, we also present the Throughput results for the CAs, for both versions of MMCG, in Table V for consistency. Thus E-MMCG CAs not only reduce the abrupt terminations of flows when compared to the respective C-MMCG versions, but also enhance the performance of a better CA scheme, MaIS-CA here, when compared to a less efficient algorithm such as BFS-CA.

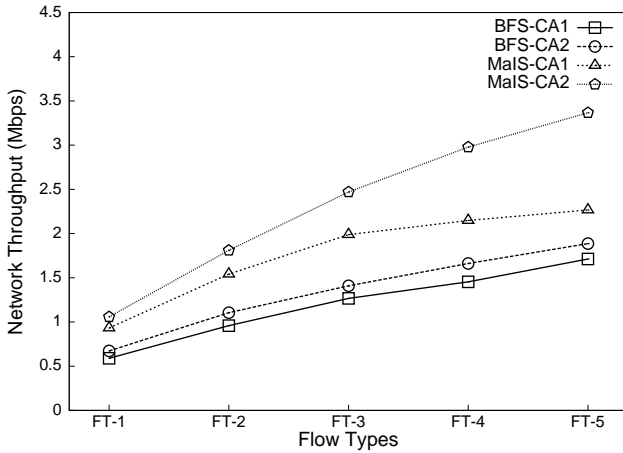


Fig. 8: Throughput in Test Case Class 2

6.4.2. Test Case Class 2:

We now focus on, and analyze the response of the CA deployments in the WMN in terms of observed throughput, as new four-hop flows are injected in the network. Results of *Test Case Class 2*, which consists of a variety of multi-hop test cases, are exhibited as a graph in Figure 8. The throughput recorded for each of the five test cases in this class, represented by $FT-Y$, where $Y \in \{1...5\}$, is plotted for the four CA schemes. It is clearly evident that the E-MMCG version of a CA outperforms the C-MMCG version by a significant margin. For a reference, we quote the statistics of FT-5 from

Figure 8, for all the four CAs. The throughput values of BFS-CA₁, BFS-CA₂, MaIS-CA₁, and MaIS-CA₂, are recorded to be *1.711 Mbps*, *1.88 Mbps*, *2.26 Mbps* and *3.36 Mbps*, respectively. We process the results to obtain the change, *i.e.*, increase or decrease, in the observed throughput values of the two variants of the same CA, in Table VI. The throughput value of the C-MMCG version of a CA is considered as the base. A decrease, if observed, is preceded by a negative sign.

TABLE VI: % Change in Throughput Values of an E-MMCG CA over corresponding C-MMCG CA in Test Case Class 2

CA Strategy	% Change in Throughput in FT				
	1	2	3	4	5
BFS	13.9	15.2	11.2	14.3	10.2
MaIS	13.4	17.4	24.2	38.7	48.5

Throughput values of BFS-CA₂ are higher than those of BFS-CA₁ for all Flow Types, however always within the modest range of 10% to 15.2%. The maximum observed increase is 15.2% in FT-2. A more inspiring increase in throughput can be noticed in MaIS-CA₂ with respect to MaIS-CA₁. The rise in throughput values ranges from 13.4% in FT-1, to a maximum of 48.5% in FT-5. This increase in throughput of MaIS-CA₂, continues to rise from Flow Type-1 to Flow Type-5, *i.e.*, with the increase in the number of concurrent flows injected in the network. The second objective is to assess how the two CA schemes fare against one another, in both the MMCG models. It is a rather conspicuous inference that MaIS-CA performs substantially better than BFS-CA, irrespective of the MMCG model. However, it is of great interest and relevance to study the variation of the difference in throughput values recorded for the two CA schemes, in the two MMCG models. Thus, we compute the % difference in throughput values of BFS-CA and MaIS-CA for each MMCG model in Table VII. Throughput values of BFS-CA are considered as the base, and the % increase or decrease of MaIS-CA over BFS-CA is calculated, for the particular MMCG variant. A % decrease,

if observed, is preceded by a negative sign.

TABLE VII: % Difference in Throughput Values of BFS-CA and MaIS-CA for an MMCG approach in Test Case Class 2

MMCG Model	% Difference in Throughput in FT				
	1	2	3	4	5
C-MMCG	58.1	60.7	56.8	47.7	32.3
E-MMCG	57.4	63.7	75.3	79.2	78.4
Relative Difference (%)	-1.2	4.9	32.5	66	142

In the C-MMCG deployment, MaIS-CA₁ records a significant increase over BFS-CA₁ that falls in the range of 32.3% to 60.7%. However, in the E-MMCG deployment, MaIS-CA₂ surpasses its C-MMCG variant, registering tremendous increase over BFS-CA₂ throughputs, within the range of 57.4% to 79.2%. Further, we calculate the *relative difference* of the increase in throughput that MaIS-CA shows over BFS-CA, between the two MMCG models, as a % with C-MMCG as the base. The relative difference is slightly negative at -1.2% , for FT-1 *i.e.*, the test case with one 4-HHF active at a time. However, this result is not unsettling for two simple reasons. First, that FT-1 is a minimalistic test scenario with just one 4-HHF active in a simulation, and second being the diminished magnitude of this relative decrease. Besides, the % relative difference, or rather increase, rises immensely from FT-2 through FT-5, to reach a high of 142% at FT-5, which is the most comprehensive interference scenario.

6.4.3. Test Case Class 3:

As stated in its description, this class of test-cases is aimed at measuring the network performance, in terms of network capacity, packet loss ratio and mean delay under heavy network data traffic. The Throughput results of the *stress testing* exercise are presented for analysis in the graphs depicted in Figure 9. Although the overall performance of E-MMCG CAs continues to be better than their corresponding C-MMCG peers, we can observe a few deviations from the trend. In

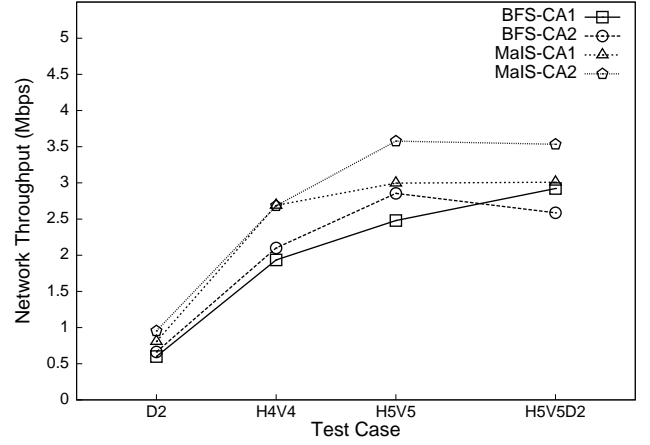


Fig. 9: Throughput in Test Case Class 3

test-case H4V4, MaIS-CA₁ registers a higher throughput than MaIS-CA₂ though by an insignificant margin of 0.24% while in the peak load scenario *i.e* H5V5D2, the throughput of BFS-CA₁ is higher than that of BFS-CA₂ by 11.4%, which can be noticed in Table VIII. The two instances in which a C-MMCG CA performs equal to or better than the corresponding E-MMCG CA do not raise any doubts about the efficacy of the E-MMCG model, but instead highlight the temporal and spatial characteristics of the endemic interference. Even a reasonably good CA may register a sub-par performance for a particular traffic scenario. In all the remaining test cases, the E-MMCG CAs outperform their C-MMCG counterparts, registering noticeable increase in throughput that falls within the range of 8.4% to 19.3%, thereby asserting their supremacy.

TABLE VIII: % Change in Throughput Values of an E-MMCG CA over corresponding C-MMCG CA in Test Case Class 3

CA Strategy	% Change in Throughput in Test Case			
	D2	H4V4	H5V5	H5V5D2
BFS	10.4	8.4	15.1	-11.4
MaIS	18.2	-0.2	19.3	17.4

Let us now examine how the two CA schemes fare against one another, in both the MMCG models. In Table IX, the % difference in throughput values of BFS-CA and MaIS-CA for each MMCG model is computed. As stated earlier, the aim is to illustrate the variation of the difference in throughput values

recorded for the two CA schemes, in the two MMCG models. MaIS-CA proves to be better than BFS-CA, regardless of the MMCG model employed. Secondly, the % change in the E-MMCG CAs is more pronounced in all scenarios except for the test-case H4V4, where this difference somewhat diminishes to 27.8% from 39% in case of C-MMCG model. This reversal is the outcome of both versions of MaIS-CA *viz.* MaIS-CA₁ and MaIS-CA₂, demonstrating similar throughput characteristics in H4V4, while BFS-CA₂ registers a higher value than BFS-CA₁, as expected.

The % relative difference, of the increase in throughput that MaIS-CA shows over BFS-CA, between the two MMCG models, is positive for all test scenarios except for test-case H4V4, which is in accordance with the discussion above.

TABLE IX: % Difference in Throughput Values of BFS-CA and MaIS-CA for an MMCG approach in Test Case Class 3

CA Strategy	% Change in Throughput in Test Case			
	D2	H4V4	H5V5	H5V5D2
C-MMCG	34.6	39.0	20.8	3.0
E-MMCG	44.0	27.8	25.3	36.6
Relative Difference (%)	27.2	-28.7	21.6	1124.1

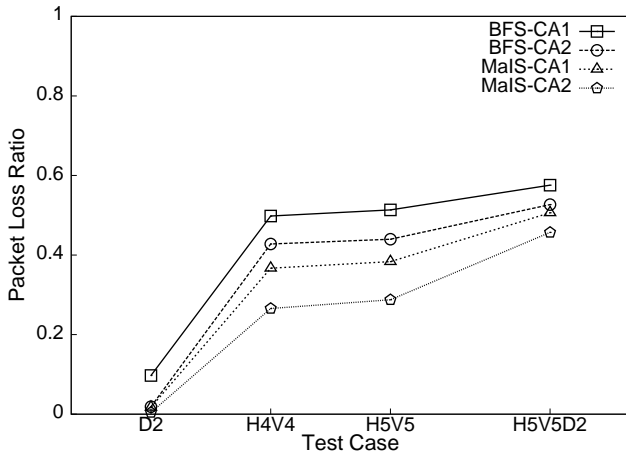


Fig. 10: Packet Loss Ratio in Test Case Class 3

Moving on to the observed PLR values, let us examine the graph in Figure 10 and the corresponding processed results in Table X. In all test-cases the E-MMCG CAs suffer a significantly lesser PLR, thereby implying a reduced impact

of endemic interference on data transmissions. In conformity with the earlier result trends, PLR results also highlight that MaIS-CA₂ registers a greater reduction in PLR over MaIS-CA₁ than BFS-CA₂ does over BFS-CA₁.

TABLE X: % Reduction in Packet Loss Ratio of an E-MMCG CA over corresponding C-MMCG CA in Test Case Class 3

CA Strategy	% Change in PLR in Test Case			
	D2	H4V4	H5V5	H5V5D2
BFS	80.7	14.1	14.3	8.4
MaIS	75.5	27.5	25.0	9.7

TABLE XI: % Difference in Packet Loss Ratio between BFS-CA and MaIS-CA for an MMCG approach in Test Case Class 3

CA Strategy	% Change in PLR in Test Case			
	D2	H4V4	H5V5	H5V5D2
C-MMCG	82.0	26.3	25.3	12.0
E-MMCG	77.1	37.8	34.6	13.2
Relative Difference (%)	-5.9	43.7	36.7	10.1

The % relative difference of decrease in PLR values that MaIS-CA shows over BFS-CA, between the two MMCG models, is positive for all values except D2 where it is -5.9% . For the remaining test-cases the relative difference is positive, always above 10% and as high as 43%. Thus we can infer that the E-MMCG model accentuates the decrease in PLR registered by MaIS-CA over BFS-CA, as compared to the C-MMCG model where this decrease is less prominent. The final metric of interest here is the mean delay (MD), the recorded results for which are depicted in the graph in Figure 11. Deviating from the pattern of other metrics, MaIS-CA does not command a clear advantage over BFS-CA. In fact the observed values for the two CAs fluctuate and can not be compared, which is easily discernible from Figure 11. However, for most test-scenarios BFS-CA₂ does register the minimum MD values performing better than even MaIS-CA₂. We restrict our analysis here to the reduction in MD that an E-MMCG CA registers over its corresponding C-MMCG CA, the processed results for which are presented in Table XII.

Both MaIS-CA₂ and BFS-CA₂ boast of a reduced MD than MaIS-CA₁ and BFS-CA₁. However, the difference between the two versions of BFS-CA is more pronounced which is a shift from the observed result pattern thus far. Nevertheless, the E-MMCG CAs succeed in reducing packet delay times in the WMN as compared to their conventional counterparts.

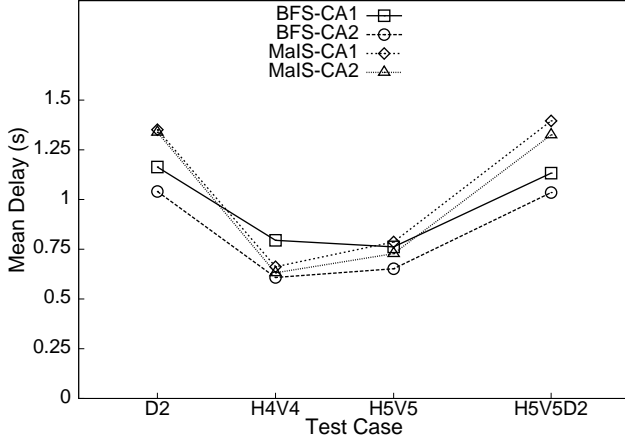


Fig. 11: Mean Delay in Test Case Class 3

TABLE XII: % Reduction in Mean Delay of an E-MMCG CA over corresponding C-MMCG CA in Test Case Class 3

CA Strategy	% Change in MD in Test Case			
	D2	H4V4	H5V5	H5V5D2
BFS	10.5	23.5	14.4	8.6
MaIS	1.0	4.5	7.4	5.0

Having stated the results of the testing effort, we now make reasonable inferences and logical conclusions. But before that, we make an observation regarding *TID* in the next subsection.

6.5. Total Interference Degree : Reliable Theoretical Metric ?

Based on the results and the subsequent analysis, we can establish the following decreasing order of precedence among the four CAs in terms of the observed performance metrics : MaIS-CA₂ > MaIS-CA₁ > BFS-CA₂ > BFS-CA₁.

The theoretical concept of *Interference Degree*, both *local*, i.e., of an individual node, and *total*, i.e., of a CA scheme in entirety, has been generously used in the WMN research literature to efficiently solve research problems such as the

CA problem, the routing problem etc. With respect to the CA problem, the guiding idea is that a CA with lesser *total interference degree* or TID, will be more efficient and register better performance as compared to a CA with a higher TID. However, we have witnessed that this theoretical idea does not necessarily hold true when compared to the actual experimental data. In any domain relying primarily on experimentation and actual deployments, the proposed theories are seldom accurate or precise, and there is a certain threshold of acceptable deviation from the theoretical predictions. However, in the case of TID of CAs, we contend that the reasonable threshold of acceptance is breached. In this section, we state and elaborate upon this anomaly.

Let us observe Table III again, and consider the TID values for the 5×5 grid. We had earlier compared the TIDs of two CAs belonging to the same MMCG model, and made theoretical inferences. But if we instead consider all four TID values, irrespective of the MMCG model, the theoretical order of precedence in the expected performance would be, MaIS-CA₁ > BFS-CA₁ > MaIS-CA₂ > BFS-CA₂, which is not in conformity with the established experimental sequence. One may present a counter-argument, that since a particular MMCG model was employed to compute the TIDs only for the CAs of the same model, a comparison of cross-model TID values is not logical. Hence, for a consistency in the approach taken to generate TID values, we employ the following two alternative methods to generate the TID values for all four CAs, regardless of the MMCG model they belong to.

- Compute TIDs using the C-MMCG algorithm.
- Compute TIDs using the E-MMCG algorithm.

We plot the TID values obtained, for FT-5 of *Test Case Class 2*, against the throughput values recorded for the CAs, in Figure 12. The titles *C-MMCG* and *E-MMCG* represent the TIDs generated using the C-MMCG and the E-MMCG algorithm, respectively. The $(TID, Throughput)$ co-ordinates for the

CA quartet, MaIS-CA₁, MaIS-CA₂, BFS-CA₁, BFS-CA₂ are labeled as *M1*, *M2*, *B1* and *B2*, respectively. Further, for clarity, the C-MMCG CA labels are prefixed by a 'c', and the E-MMCG CA labels are prefixed by an 'e'.

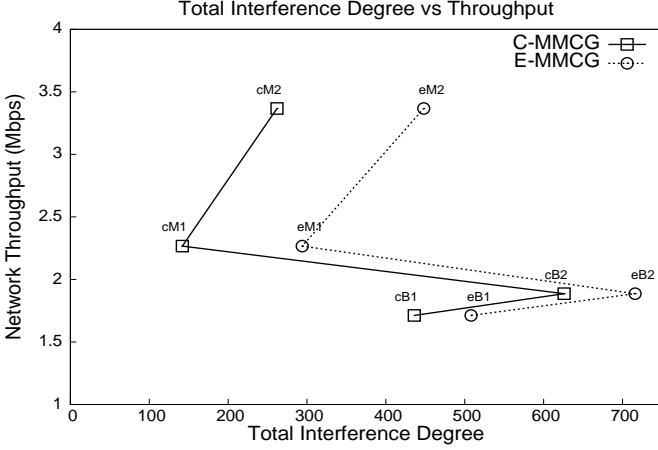


Fig. 12: Correlation of TID with Average Network Aggregate Throughput for FT-5

The plots for both the MMCG models are almost identical in shape and gradient, only differing in terms of the TID values. The E-MMCG CA versions register higher value of TIDs, which is expected as the model factors in the *RCI*. The order of CA precedence, with the TID values as the theoretical metric of performance, is the same for both methods, which is, MaIS-CA₁ > MaIS-CA₂ > BFS-CA₁ > BFS-CA₂. Ideally, the theoretical concept would dictate that the throughput decrease consistently with the rise in TID values, though not necessarily in a linear fashion. The two plots, however, adhere to no such pattern and the conspicuous deviation raises a valid concern about TID being a reliable theoretical metric to predict the performance of a CA.

The theoretical concept of *Interference Degree*, holds great relevance in understanding and estimating the prevalent interference at a node, or in the entire WMN. But extending this concept to compute *TID* for a particular CA in a WMN, and making predictions on the expected behavior or performance of a CA, based on the estimated TID values, does not appear to be a practically accurate approach. This finding has some pro-

found implications, as numerous CA approaches for WMNs have been suggested in research works, that are predicated on this theoretical concept. The underlying idea in most of these interference-aware CA approaches, e.g [27] and [28], is to minimize the local interference degree at a node, or minimize the TID while assigning channels to WMN radios.

However, the task of ascertaining the benefit and relevance of predicating CA design of a WMN on its TID is beyond the scope of our current work.

7. CONCLUSIONS AND INFERENCES

We begin by drawing the most fundamental conclusion that *RCI* has a rather debilitating effect on the performance of WMNs. It is safe to conclude that the *Enhanced MMCG* model, which factors in, and adequately represents, the interference generated by SCRs, is better equipped and algorithmically more tuned to alleviate the adverse impact of interference, than its conventional counterpart, the *Classical MMCG* model. In addition to the above conclusions, there are a few insightful inferences that we make based on the observed results.

CA deployments under the E-MMCG class invariably perform better than their peers under the C-MMCG approach, for all the performance indices. The improvement noticed in MaIS-CA is substantial as compared to BFS-CA. Therefore, though the E-MMCG model augments the performance metrics of a CA, the underlying CA strategy also plays a determining role in this enhancement. This inference is a positive feature of the E-MMCG model, in the way that it does not alter or modify the inherent behavior or algorithmic nature of a CA. Simply put, if a CA approach is fundamentally good or bad, although its performance is enhanced by the E-MMCG model, it will continue to be *relatively* good or bad.

The third observation is that the *Relative Difference* of the performance between the two CA schemes, under the two

MMCG approaches, is not just positive in favor of E-MMCG, but boasts of high magnitudes as well. The E-MMCG model accentuates the difference between the performance metrics of two CA schemes, in a positive fashion, *i.e.*, a less efficient CA scheme will be enhanced marginally (e.g. BFS-CA) while an intelligent CA stands to gain drastically (e.g. MaIS-CA) from the E-MMCG model. Naively put, bad becomes less bad, but good becomes much better.

On the subject of *TID* as a theoretical estimate of the endemic interference in a WMN, the inference from the discussion asserts that it is not an ideal metric, especially when used to predict the behavior of a deployed CA.

8. FUTURE WORK

Having established the notion of *RCI* and experimentally validated it, we plan to further explore the concept to engineer a radio co-location aware channel assignment. We also intend to take up the task of determining a better theoretical metric for estimating the impact of interference in a WMN.

9. COMPLIANCE WITH ETHICAL STANDARDS

9.1. Conflict of Interest

The authors declare that they have no conflict of interest.

9.2. Research involving human participants and/or animals

This chapter does not contain any studies with human participants or animals performed by any of the authors.

9.3. Informed Consent

No Individual Participants were a part of this study, nor was any personal data collected. Hence Informed Consent is not applicable to this study.

REFERENCES

- [1] I. F. Akyildiz and X. Wang, "A survey on wireless mesh networks," *Communications Magazine, IEEE*, vol. 43, no. 9, pp. S23–S30, 2005.
- [2] R. Bruno, M. Conti, and E. Gregori, "Mesh networks: commodity multihop ad hoc networks," *Communications Magazine, IEEE*, vol. 43, no. 3, pp. 123–131, 2005.
- [3] A. Capone, G. Carello, I. Filippini, S. Gualandi, and F. Malucelli, "Routing, scheduling and channel assignment in wireless mesh networks: optimization models and algorithms," *Ad Hoc Networks*, vol. 8, no. 6, pp. 545–563, 2010.
- [4] H. Skalli, S. Ghosh, S. K. Das, L. Lenzini, and M. Conti, "Channel assignment strategies for multiradio wireless mesh networks: issues and solutions," *Communications Magazine, IEEE*, vol. 45, no. 11, pp. 86–95, 2007.
- [5] I. F. Akyildiz, X. Wang, and W. Wang, "Wireless mesh networks: a survey," *Computer networks*, vol. 47, no. 4, pp. 445–487, 2005.
- [6] I. . W. Group *et al.*, "Ieee standard for information technology–telecommunications and information exchange between systems–local and metropolitan area networks–specific requirements–part 11: Wireless lan medium access control (mac) and physical layer (phy) specifications amendment 6: Wireless access in vehicular environments," *IEEE Std*, vol. 802, p. 11p, 2010.
- [7] P. Gupta and P. R. Kumar, "The capacity of wireless networks," *Information Theory, IEEE Transactions on*, vol. 46, no. 2, pp. 388–404, 2000.
- [8] S. Xu and T. Saadawi, "Does the ieee 802.11 mac protocol work well in multihop wireless ad hoc networks?" *Communications Magazine, IEEE*, vol. 39, no. 6, pp. 130–137, 2001.
- [9] W. Si, S. Selvakenedy, and A. Y. Zomaya, "An overview of channel assignment methods for multi-radio multi-channel wireless mesh networks," *Journal of Parallel and Distributed Computing*, vol. 70, no. 5, pp. 505–524, 2010.
- [10] A. Raniwala and T.-c. Chiueh, "Architecture and algorithms for an ieee 802.11-based multi-channel wireless mesh network," in *INFOCOM 2005. 24th Annual Joint Conference of the IEEE Computer and Communications Societies. Proceedings IEEE*, vol. 3. IEEE, 2005, pp. 2223–2234.
- [11] MeshDynamics, "MeshDynamics Technology-Performance analysis, url=<http://www.meshdynamics.com>," 2006.
- [12] S. M. Das, D. Koutsonikolas, Y. C. Hu, and D. Peroulis, "Characterizing multi-way interference in wireless mesh networks," in *Proceedings of the 1st international workshop on Wireless network testbeds, experimental evaluation & characterization*. ACM, 2006, pp. 57–64.
- [13] A. Iyer, C. Rosenberg, and A. Karnik, "What is the right model for wireless channel interference?" *Wireless Communications, IEEE Transactions on*, vol. 8, no. 5, pp. 2662–2671, 2009.

- [14] P. Cardieri, "Modeling interference in wireless ad hoc networks," *Communications Surveys & Tutorials, IEEE*, vol. 12, no. 4, pp. 551–572, 2010.
- [15] K. N. Ramachandran, E. M. Belding-Royer, K. C. Almeroth, and M. M. Buddhikot, "Interference-aware channel assignment in multi-radio wireless mesh networks," in *INFOCOM*, vol. 6, 2006, pp. 1–12.
- [16] J. Crichigno, M.-Y. Wu, and W. Shu, "Protocols and architectures for channel assignment in wireless mesh networks," *Ad Hoc Networks*, vol. 6, no. 7, pp. 1051–1077, 2008.
- [17] A. P. Subramanian, H. Gupta, S. R. Das, and J. Cao, "Minimum interference channel assignment in multiradio wireless mesh networks," *Mobile Computing, IEEE Transactions on*, vol. 7, no. 12, pp. 1459–1473, 2008.
- [18] Y. Xutao and X. Jin, "A channel assignment method for multi-channel static wireless networks," in *2011 Global Mobile Congress*, 2011, pp. 1–4.
- [19] M. K. Marina, S. R. Das, and A. P. Subramanian, "A topology control approach for utilizing multiple channels in multi-radio wireless mesh networks," *Computer networks*, vol. 54, no. 2, pp. 241–256, 2010.
- [20] L. Cao and M.-Y. Wu, "Upper bound of the number of channels for conflict-free communication in multi-channel wireless networks," in *Wireless Communications and Networking Conference, 2007. WCNC 2007. IEEE*. IEEE, 2007, pp. 2032–2037.
- [21] H. Li, Y. Cheng, C. Zhou, and P. Wan, "Multi-dimensional conflict graph based computing for optimal capacity in mr-mc wireless networks," in *Distributed Computing Systems (ICDCS), 2010 IEEE 30th International Conference on*. IEEE, 2010, pp. 774–783.
- [22] A. H. M. Rad and V. W. Wong, "Joint channel allocation, interface assignment and mac design for multi-channel wireless mesh networks," in *INFOCOM 2007. 26th IEEE International Conference on Computer Communications. IEEE*. IEEE, 2007, pp. 1469–1477.
- [23] H. Cheng, G. Chen, N. Xiong, and X. Zhuang, "Static channel assignment algorithm in multi-channel wireless mesh networks," in *Cyber-Enabled Distributed Computing and Knowledge Discovery, 2009. CyberC'09. International Conference on*. IEEE, 2009, pp. 49–55.
- [24] A. U. Chaudhry, J. W. Chinneck, and R. H. Hafez, "Channel requirements for interference-free wireless mesh networks to achieve maximum throughput," in *Computer Communications and Networks (ICCCN), 2013 22nd International Conference on*. IEEE, 2013, pp. 1–7.
- [25] T. R. Henderson, M. Lacage, G. F. Riley, C. Dowell, and J. Kopena, "Network simulations with the ns-3 simulator," *SIGCOMM demonstration*, 2008.
- [26] A. M. Al-Jubari, M. Othman, B. M. Ali, and N. A. W. A. Hamid, "Tcp performance in multi-hop wireless ad hoc networks: challenges and solution," *EURASIP Journal on Wireless Communications and Networking*, vol. 2011, no. 1, pp. 1–25, 2011.
- [27] Y. Ding and L. Xiao, "Channel allocation in multi-channel wireless mesh networks," *Computer Communications*, vol. 34, no. 7, pp. 803–815, 2011.
- [28] A. Sen, S. Murthy, S. Ganguly, and S. Bhatnagar, "An interference-aware channel assignment scheme for wireless mesh networks," in *Communications, 2007. ICC'07. IEEE International Conference on*. IEEE, 2007, pp. 3471–3476.